Self-Assembly of a Colloidal Interstitial Solid with Tunable Sublattice Doping

L. Filion, M. Hermes, R. Ni, E. C. M. Vermolen, A. Kuijk, C. G. Christova, J. C. P. Stiefelhagen, T. Vissers, A. van Blaaderen, and M. Dijkstra

Soft Condensed Matter, Debye Institute for NanoMaterials Science, Utrecht University, Princetonplein 1, NL-3584 CC Utrecht, the Netherlands

(Received 16 May 2011; published 11 October 2011)

We determine the phase diagram of a binary mixture of small and large hard spheres with a size ratio of 0.3 using free-energy calculations in Monte Carlo simulations. We find a stable binary fluid phase, a pure face-centered-cubic (fcc) crystal phase of the small spheres, and binary crystal structures with LS and LS_6 stoichiometries. Surprisingly, we demonstrate theoretically and experimentally the stability of a novel interstitial solid solution in binary hard-sphere mixtures, which is constructed by filling the octahedral holes of an fcc crystal of large spheres with small spheres. We find that the fraction of octahedral holes filled with a small sphere can be completely tuned from 0 to 1. Additionally, we study the hopping of the small spheres between neighboring octahedral holes, and interestingly, we find that the diffusion increases upon increasing the density of small spheres.

DOI: 10.1103/PhysRevLett.107.168302 PACS numbers: 82.70.Dd, 61.50.Ah, 81.30.Dz

Our understanding of the structure and phase behavior in colloidal and nanoparticle systems relies greatly on our knowledge of the hard-sphere system, which can be considered as a reference system for more realistic systems. While interactions between such colloids and nanoparticles are complicated, due to, e.g., van der Waals interactions, steric stabilization, electrostatics, and depletion effects, systems can often be constructed where these interactions are minimized and the particles behave like hard particles, e.g., Refs. [1–3]. One of the first observations of binary crystal structures in colloidal systems was made by Murray and Sanders in naturally occuring Brazilian gem opals [4]. The structures they identified have since been shown to be stable in binary hard-sphere mixtures [5]. More generally, theoretical and experimental studies of binary mixtures of hard spheres have found regions of stability for binary liquids, monodisperse face-centered-cubic (fcc) crystals, binary crystal phases NaCl, $NaZn_{13}$, AlB_2, and $MgZn_2$, and substitional solids [5–8].

In this Letter, we demonstrate theoretically and experimentally the self-assembly of a novel thermodynamically stable interstitial solid solution (ISS) in a binary mixture of hard spheres, which is constructed by filling the octahedral holes of an fcc crystal of the large particles with small particles. In an ISS phase, instead of both species ordering on a binary crystal lattice, only one of the species is properly ordered on a lattice, while the other species is placed irregularily on a sublattice. The resulting ISS phase can be seen as a compromise between a binary crystal where both species have crystalline order and a crystal phase of only large particles in coexistence with a disordered fluid phase, and is hence a truly ''interstitial'' solution to the problem of maximizing entropy. The ISS phase is found in atomic systems; e.g., crystalline iron is strengthened by the addition of interstitial carbon atoms yielding steel. However, to the best of our knowledge, a thermodynamically stable ISS phase has not been reported in colloidal and nanoparticle mixtures. Surprisingly, we find that the fraction of octahedral holes filled with a small particle can be completely tuned from 0 to 1. We are unaware of another (atomic) system which shows a completely tunable ISS phase. That entropy alone can stabilize an ISS phase is not trivial, as the presence of the small particles may affect the stability of the underlying crystal lattice of large particles.

To demonstrate the stability of the ISS phase, we consider a binary mixture of large and small spheres with diameters σ_L and σ_S respectively, and size ratio $q = \sigma_S/\sigma_L = 0.3$. Following Ref. [9], we first predict the candidate binary crystal structures for this mixture where both species exhibit long-range crystalline order. We find NaCl, NiAs, and a superlattice structure with LS_6 stoichiometry where L (S) represents the large (small) particles (Fig. 1 and Supp. Fig. S1 [10]). We also examined larger systems using kinetic Monte Carlo simulations [11] and found an ISS nucleus formed spontaneously indicating that a fcc-based ISS phase should also be considered a candidate phase. We point out that a NaCl structure is constructed by filling every octahedral hole in an fcc lattice of large particles with a single small particle (Fig. 1). Thus, a random, incomplete filling trivially results in an ISS. The stoichiometry of the ISS phase is defined as LS_n where n is a fractional number in the range [0, 1]. We note that $n = 0$ corresponds to the fcc phase and $n = 1$ to a perfect NaCl structure where the small particles are also on an fcc lattice. An ISS phase can also be constructed by filling some octahedral holes in the monodisperse HCP lattice; a complete filling yields a NiAs structure. However, the pure fcc and binary NaCl structures are more stable for hard spheres than the competing HCP and NiAs phases with free-energy

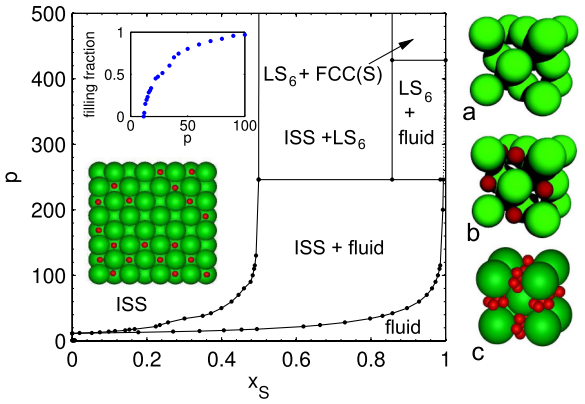

FIG. 1 (color online). Left: Phase diagram of the binary hard-sphere mixture in the composition $x_s = N_S/(N_S + N_L)$-reduced pressure $p = \beta P \sigma_L^3$ plane. The stable one-phase regions labeled "ISS" and "fluid" denote the interstitial solid solution and the binary fluid consisting of large and small particles. The labels "ISS + fluid", "LS_6 + fluid", "ISS + LS_6", and "LS_6 + FCC(S)" denote the coexistence regions where the tie-lines that connect the two coexisting phases are horizontal. fcc(S) denotes a face-centered cubic crystal of the small spheres. Inset: The stoichiometry n of the coexisting ISS phase as a function of the pressure. A typical configuration of an ISS with localized interstitials is also displayed. Right: Unit cells of (a) fcc, (b) NaCl and (c) the LS_6 crystal structure. Note that NaCl is constructed by filling the octahedral holes in the fcc lattice of large particles with small particles.

differences on the order of 0.001 k_BT [12] and 0.002 k_BT [13] per particle, respectively. Here k_B denotes Boltzmann's constant and T the absolute temperature. We stress that experimentally, the presence of interstitials in the holes of the fcc lattice can stem from two main causes: (i) a lowering of the free energy due to the addition of the interstitials resulting in a thermodynamically stable ISS phase, or (ii) a kinetic trapping of the interstitials leading to nonequilibrium crystal structures. While these two effects are often difficult to distinguish experimentally, free-energy calculations using computer simulations can demonstrate conclusively whether or not ISS phases are stable compared to fcc crystals of the large and small spheres and the binary liquid.

To determine the phase behavior of this system, we calculate the free-energy of the binary NaCl phase, the LS_6 phase, the binary liquid phase, pure fcc phases of small and large spheres and the ISS phase. The Gibbs free energies for the binary fluid and fcc phases were taken from previous studies [14], while the Gibbs free energies of the NaCl crystal and LS_6 crystal structures were calculated using Einstein integration as in Ref. [6]. For the interstitial solid we employ the identity [15]

$$F(N_L, z_S, V) = F(N_L, z_S = 0, V) - \int_0^{z_S} dz_S' \frac{\langle N_S \rangle_{z_S'}}{z_S'},$$

where $F(N_L, z_S, V)$ denotes the thermodynamic potential corresponding to the (N_L, z_S, V) ensemble, the first term at the right-hand side is the free-energy of the pure large sphere fcc phase, and the integrand in the second term can be determined from measuring the average number of absorbed small particles from a reservoir at fugacity z_S onto a system of N_L large spheres in a volume V. Monte Carlo (MC) simulations in the NPT ensemble were used to determine the equation of state. In the case of the ISS we included large displacement moves of the small particles in addition to typical MC particle moves in order to allow them to move from one octahedral hole to another and thus average over the disorder induced by the small particles. All calculations were performed on 256 to 4000 particles. Using common tangent constructions of the Gibbs free energies at constant pressure we determined the coexistence regions and constructed the phase diagram. The phase diagram in the pressure-composition (p-x_S) representation is shown in Fig. 1, where $p = \beta P \sigma_L^3$ is the reduced pressure, $x_S = N_S/(N_S + N_L)$, $N_{S(L)}$ is the number of small (large) hard spheres, $\beta = 1/k_BT$ and V is the volume. From Fig. 1 we see that there is a large region of parameter space where the ISS phase is stable. Additionally, the inset in Fig. 1 demonstrates how the filling of the octahedral holes with small particles in the coexisting ISS increases as a function of pressure, slowly approaching the stoichiometry $n = 1$ of NaCl.

As an illustration of the experimental accessibility of the ISS phase, we performed sedimentation experiments using core-shell silica colloids. The structural and thermodynamic properties of a system under gravity at a certain height are the same as those of a bulk system at the corresponding pressure. Sedimentation experiments are therefore often used in scanning the properties of a system over a range of pressures in a single experiment [16]. Typical snapshots obtained by confocal microscopy are shown in Fig. 2 and Supp. Fig. S3 [10]. The confocal image in Fig. 2 depicts an experimental realization of an ISS with stoichiometry $n \simeq 0.3$. We find that the concentration of small particles decreases as a function of height in the sample (Fig. 2) which is in qualitative agreement with the phase diagram which predicts an increasing concentration of small particles with pressure. The confocal images and height profile demonstrate not only the existence of the ISS in this system, but the large range over which the stoichiometry n of the ISS can be tuned. However, we did not observe the LS_6 superlattice structure as this occurs at high pressures where it is difficult to observe equilibrium behavior experimentally. Furthermore, in examining the motion of the small particles using confocal microscopy, we noted that some small particles near the top of the sample were moving between interstitial lattice sites. Near the bottom of the sample, this was not observed. Motivated by this intriguing observation, we examined the motion of the small particles in an ISS phase in more detail using event driven MD simulations [17]. In these simulations the large (small) particles had a mass

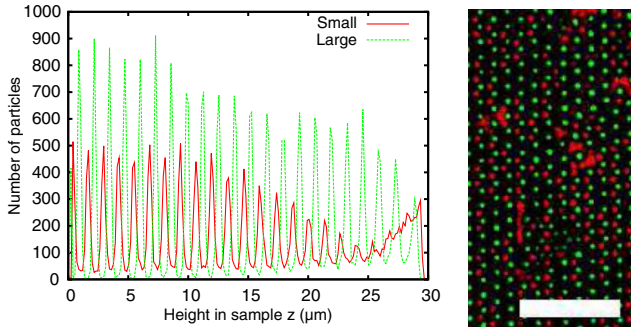

FIG. 2 (color online). Left: The density profiles of the small and large particles from a sedimentation experiment. Right: Confocal image of an interstitial solid solution with size ratio $q = 0.3$ and $n \simeq 0.3$ In this image two (111) planes of the crystal, one consisting of mostly small (red) particles with the other consisting of mostly large (green) particles have been overlayed in order to be viewable in the same figure. The larger and darker red regions correspond to defects, such as vacancies, in the underlying lattice of green particles which have been filled by many small (red) particles. Scale bar is 10 μm.

$m_L(m_S)$, where $m_S = m_L\sigma_S^3/\sigma_L^3$, and time was measured in units of $\sigma_L\sqrt{m_L/(k_BT)}$. The initial velocities were drawn randomly from a Maxwell-Boltzmann distribution after which the center of mass was fixed. A typical trajectory taken by a single small particle is shown in Fig. 3 which demonstrates clearly that the particles spend most of their time in the octahedral holes of the lattice. However, the particles do not hop directly between the octahedral holes but rather hop via a neighboring tetrahedral hole in the fcc lattice. We point out that the tetrahedral holes are significantly smaller than the octahedral holes, $0.225\sigma_L$ in comparison to $0.414\sigma_L$ at close packing.

At close packing of the underlying fcc crystal, the interstitials are prevented from moving between neighboring holes by the presence of the large particles. However, at lower pressures due to larger lattice constants in combination with the motion of large particles around their lattice sites (phonons), the small particles can travel between the octahedral holes. We calculated the mean square displacement (MSD) $\langle\Delta r_S^2(t)\rangle$ of the small particles as a function of time. From this MSD, we determined the long-time self-diffusion constant of the small particles (D) as a function of number density for various stoichiometries (Fig. 3). As evident in Fig. 3, D increases with stoichiometry n when the number density of the large particles is kept fixed. This is in contrast to most systems where the diffusion constant decreases with density; in general as the density increases the available space in the system decreases leaving less room for particles to move resulting in a lower diffusion constant. However, in this case, as the number of small particles in the system is increased, the mean square displacement of the large particles from their ideal lattice sites increases (Supp. Fig. S5 [10]), likely arising from an increase in the depletion interaction. This in turn lowers

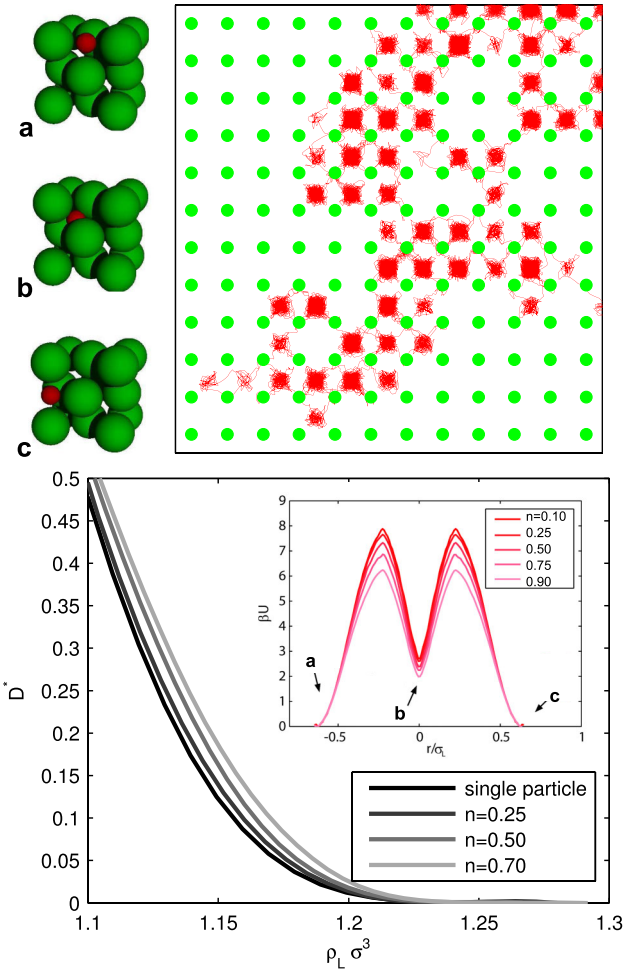

FIG. 3 (color online). Top: The trajectory of a single particle for a volume fraction of the large particles $\eta_L = 0.6$. Note that the trajectories connecting the lattice sites are neither vertical nor horizontal indicating that the small particle does not take the direct route between neighboring holes, but rather hops first to a tetrahedral hole, and then to an octahedral hole. A cartoon depicting this process is shown on the left. Bottom: Dimensionless, long-time self-diffusion coefficient $D^* = D\sqrt{\beta m_L}/\sigma_L$ as a function of the number density of large particles ($\rho_L\sigma_L^3$) for various interstitial solid solution stoichiometries n. Note that the D^* increases with stoichiometry n. Inset: Free-energy barriers in an interstitial solid solution felt by small particles hopping from an octahedral hole to a tetragonal hole and back to an octahedral hole for $\eta_L = 0.6$. Note that the height of the free-energy barriers decreases as a function of stoichiometry (filling fraction) n.

the free-energy barrier between octahedral and tetragonal sites (Fig. 3) leading to an increase of the diffusion coefficient of the small spheres. The free-energy barriers were calculated using event driven MD simulations with $N_L = 864$ large particles. Each small particle coordinate was mapped to the closest position on the line connecting the ideal lattice positions of an octahedral hole with a tetragonal hole and the probability ($P(x)$) of finding a small particle at position x along that line was determined.

The free-energy barrier was then determined from $\beta U(x) = -\log P(x)$.

The phase behavior of this system can be compared to previous experimental and theoretical studies of binary hard-sphere mixtures. Vermolen *et al.* examined various methods for growing binary NaCl hard-sphere crystals including gravitational and electric fields, epitaxial templates, and dielectrophoretic compression from a binary mixture with size ratio $q = 0.3$ [13]. However, the crystal structures they found all included a significant number of vacancies of the small colloids ($> 10\%$). This result is in keeping with the phase behavior observed in Fig. 1. Hunt *et al.* also examined binary hard-sphere mixtures of particles with $q = 0.39$ and 0.42 and reported the presence of NaCl [18]. However, from their presented results it is impossible to distinguish between an ISS and a NaCl crystal. On the theoretical side, the closest size ratios examined in literature using free-energy calculations are the phase diagrams presented for binary hard-sphere mixtures with $q = 0.2$ [15] and 0.414 [7]. For $q = 0.2$, the phase behavior is expected to be significantly different than that for $q = 0.3$ as the small particles can fit in both the tetragonal and octahedral holes. However, the phase behavior for a binary hard-sphere mixture with $q = 0.414$ is likely to be qualitatively the same as that of $q = 0.3$. In both cases, the smaller particles both fit and are restricted to reside in the octahedral holes at close packing. MD snapshots included in Ref. [7] for the $q = 0.414$ mixture show a coexistence between a solid and fluid phase which the authors identified as a monodisperse fcc phase and a binary liquid phase. However, the fcc phase depicted in their snapshots contains some small particles, and is more likely an ISS phase. To summarize, the NaCl phases previously identified experimentally [13] and theoretically [7] were most likely ISSs. Additionally, we remark that there are a vast number of other colloidal and nanoparticle systems which may form an ISS phase. In particular we have also found an fcc-based ISS phase in experiments on binary mixtures of oppositely charged colloids with size ratio $\sigma_S/\sigma_L = 0.73$ (Supp. Figs. S6 and S7 [10]) thereby indicating that the ISS phase is not restricted to hard-sphere systems. Moreover, we would also expect binary mixtures of charged colloids to form body-centered-cubic (BCC) based ISSs since the BCC lattice is stable for monodisperse particles interacting via a Yukawa potential.

In conclusion, we have demonstrated that the ISS is thermodynamically stable in binary hard-sphere mixtures and is likely stable for a wide variety of particle interactions. Our finding on the stability of ISS phases is of vital importance for a wide range of applications as it provides a method to grow large, defect-free single colloidal ISS crystals with unprecedented control of the sublattice doping. For instance, a transistor based on a regularly doped semiconductor has been realized with a binary nanocrystal solid [19]. Similarly, intriguing structural color tuning has previously been achieved by interstitial doping of an fcc photonic crystal with light absorbing nanoparticles [20]. Extending this to the ISS phase present in our model, we would expect more control over the color tuning. More generally, the availability of a simple model system which is both theoretically and experimentally realizable will be of great value for the understanding of the many ISS phases arising in atomic and molecular systems. The nucleation of molecular ISSs can be very complex due to the different time scales on which both species equilibrate. Realizing a stable ISS phase in a colloidal system allows one to study the nucleation process in real space on reasonable time scales. Additionally, this ISS is an ideal system for examining interactions between equilibrium interstitial defects for any concentration.

We acknowledge J. Hoogenboom for particle synthesis and F. Smallenburg and M. Marechal for fruitful discussions. We acknowledge financial support from Nanodirect, NWO-CW, a NWO-VICI grant, NanoNed, and FOM.

[1] A. Yethiraj and A. van Blaaderen, Nature (London) **421**, 513 (2003).
[2] P. N. Pusey and W. van Megen, Nature (London) **320**, 340 (1986).
[3] Z. Chen and S. O'Brien, ACS Nano **2**, 1219 (2008).
[4] J. V. Sanders and M. J. Murray, Nature (London) **275**, 201 (1978).
[5] M. D. Eldridge, P. A. Madden, and D. Frenkel, Nature (London) **365**, 35 (1993).
[6] A. Hynninen, L. Filion, and M. Dijkstra, J. Chem. Phys. **131**, 064902 (2009).
[7] E. Trizac, M. D. Eldridge, and P. A. Madden, Mol. Phys. **90**, 675 (1997).
[8] W. G. T. Kranendonk and D. Frenkel, Mol. Phys. **72**, 679 (1991).
[9] L. Filion *et al.*, Phys. Rev. Lett. **103**, 188302 (2009).
[10] See Supplemental Material at http://link.aps.org/supplemental/10.1103/PhysRevLett.107.168302 for more details.
[11] K. Kikuchi, M. Yoshida, T. Maekawa, and H. Watanabe, Chem. Phys. Lett. **185**, 335 (1991).
[12] P. G. Bolhuis, D. Frenkel, S. Mau, and D. A. Huse, Nature (London) **388**, 235 (1997).
[13] E. C. M. Vermolen *et al.*, Proc. Natl. Acad. Sci. U.S.A. **106**, 16 063 (2009).
[14] R. J. Speedy, J. Phys. Condens. Matter **10**, 4387 (1998); G. A. Mansoori, N. F. Carnahan, K. E. Starling, and J. Leland, J. Chem. Phys. **54**, 1523 (1971).
[15] M. Dijkstra, R. van Roij, and R. Evans, Phys. Rev. E **59**, 5744 (1999).
[16] R. Piazza, T. Bellini, and V. Degiorgio, Phys. Rev. Lett. **71**, 4267 (1993).
[17] B. J. Alder and T. E. Wainwright, J. Chem. Phys. **31**, 459 (1959).
[18] N. Hunt, R. Jardine, and P. Bartlett, Phys. Rev. E **62**, 900 (2000).
[19] J. J. Urban *et al.*, Nature Mater. **6**, 115 (2007).
[20] O. L. Pursiainen *et al.*, Opt. Express **15**, 9553 (2007).